Resonance Enhancement in Silicon-on-Insulator-Based Two-Ring Mach–Zehnder Interferometer

S. Darmawan, Y. M. Landobasa, P. Dumon, R. Baets, and M. K. Chin

***Abstract*—We propose and demonstrate a two-ring coupled Mach–Zehnder interferometer (2RMZI) device that exhibits a sharp resonance with background suppression to give both high finesse and modulation depth. The combination of MZI and the two-ring structure leads to more complete destructive interference that effectively removes the unwanted background envelope effect found in the transmission spectrum of a simple two-ring-two-bus (2R2B) system. The projected finesse enhancement of 2RMZI relative to one-ring coupled MZI and 2R2B is discussed based on best-fit parameter values that match the fabricated devices.**

***Index Terms*—Guided waves, high-index contrast, integrated optic devices, Mach–Zehnder, microring resonators, photonic wire, silicon-on-insulator (SOI) technology, two-ring configuration.**

I. Introduction

MICRORING resonators are flexible building blocks in photonic integrated circuits for realizing various optical functionalities such as filters, sensors, modulators, and switches. Of particular interest for sensing and switching applications is the microring-based Mach–Zehnder interferometer (MZI) structure where a single-ring is coupled to one arm of the MZI (1RMZI) to give a resonant enhancement of the phase shift in that arm [1]. Recently, the two-ring configuration was proposed by Landobasa in single-bus (2R1B) and double-bus (2R2B) excitation [2], [3]. These structures consist of two mutually coupled rings of possibly different sizes, where only one ring, referred to as the inner ring, is coupled to the bus(es), as shown in the inset of Fig. 1(a) A significant resonance narrowing is predicted and observed [3] when the size of the outer ring is twice that of the inner ring (i.e., $\gamma = 2$), which implies that the outer-ring resonance coincides with the inner-ring antiresonance (refer to the narrow resonance in Fig. 1(b) at $\delta_1 = \pi$). In such a case, the two-ring system can effectively localize the light strongly inside the outer ring, giving rise to a sharp resonance with finesse limited only by the intrinsic and coupling losses.

Manuscript received June 6, 2008; revised June 30, 2008. The work of S. Darmawan was supported by the Singapore Millennium Foundation through a scholarship.

S. Darmawan, Y. M. Landobasa, and M. K. Chin are with the School of Electrical and Electronic Engineering, Nanyang Technological University, Singapore 639798, Singapore (e-mail: emkchin@ntu.edu.sg).

P. Dumon and R. Baets are with the Photonics Research Group of the Department of Information Technology (INTEC), Ghent University-IMEC, 9000 Gent, Belgium (e-mail: Pieter.Dumon@intec.UGent.be).

Color versions of one or more of the figures in this letter are available online at http://ieeexplore.ieee.org.

Digital Object Identifier 10.1109/LPT.2008.928843

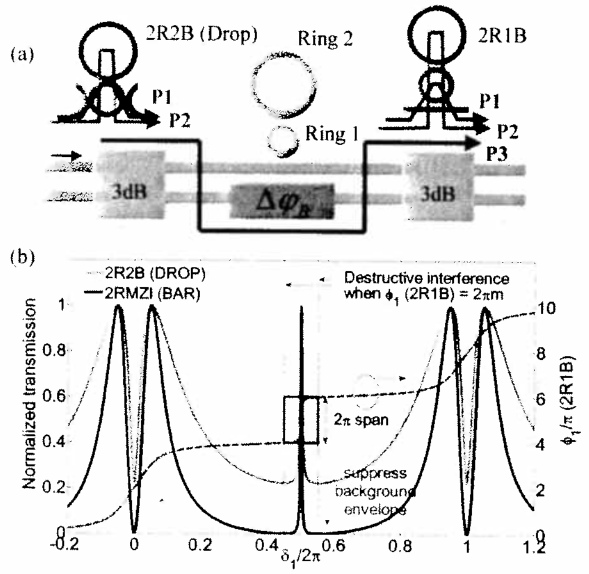

Fig. 1. (a) The 2RMZI. The left and right insets show the 2R2B and 2R1B structures and their possible optical pathways P1 and P2. The MZI provides additional optical pathway P3 for destructive interference with P1 and P2 at $\varphi_1 = 2\pi m$. (b) Transmission of 2R2B (Drop) (faded line) showing poor logic "0", the 2RMZI (Bar) (solid line), and the phase response φ_1 of 2R1B (dashed line-right axis). Simulated parameters: $r_1 \sim 0.6$, $r_2 \sim 0.9$, assuming lossless case and balanced MZI for the 2RMZI.

In the two-bus case, the finesse is lower compared to the one-bus because the coupling loss is twice as large, but it has the advantage of having two complementary outputs—through (T) and drop (D)—and hence is useful as an add–drop filter. The drop spectrum of the 2R2B structure over one full spectral range is shown in Fig. 1(b), where δ_1 is the inner ring round-trip phase. Note that the sharp narrow resonance at $\delta_1 = \pi$ (antiresonance in inner ring) corresponds to the strong resonance in the outer ring, while the broad split resonance at $\delta_1 = 2\pi$ occurs when both rings are resonant. The narrow resonance arises because of the 2π resonant phase response from the outer ring which leads to rapid successive destructive and constructive interference. However, the destructive interference is not complete, resulting in an off-resonant dip that does not go to zero. This background envelope limits the application of such narrow resonances, e.g., for switching, modulation, or sensing. For such applications, the important figures of merit are the finesse and the modulation depth (MD) or the contrast ratio (CR). The latter MD (CR) is given by the difference (ratio) between the on-resonance and off-resonance transmission values, and is reduced by the background envelope.

To alleviate this problem, we propose to excite the 2R1B with an MZI, as shown in Fig. 1(a). By doing so, we obtain

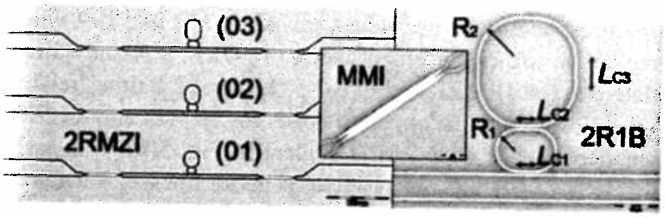

Fig. 2. Fabricated 2RMZI (left) and 2R1B (right) based on SOI. L_{C1} and L_{C2} are lengths of the DC sections of Rings 1 and 2.

three advantages: 1) The double-bus excitation is converted into single-bus excitation, giving improved light localization inside the two-ring system. 2) The output is similar to 2R2B as the MZI has both complementary cross and bar outputs. In a balanced MZI, the bar (cross) port is similar to the drop (add) port of the 2R2B. 3) The additional pathway through the MZI, shown as P3 in Fig. 1, together with the two possible pathways P1 and P2 through the 2R1B structure, allows a more complete destructive interference off the antiresonance of Ring 1 thereby giving improved CR, MD, and finesse for the narrow resonance. This is borne out by the simulated spectrum for a balanced, lossless two-ring coupled MZI (2RMZI) as shown in Fig. 1(b), where the background envelope has been significantly suppressed.

In general, however, the MZI itself may not be balanced due to fabrication variations and the presence of rings near one arm. This intrinsic asymmetry may be represented by a phase bias ($\Delta\varphi_B$) in the other arm. The 2RMZI outputs are then given by

$$T_{\mathrm{BAR}} = \left|\frac{[t_1 - \exp(i\Delta\phi_B)]}{2}\right|^2$$
$$T_{\mathrm{CROSS}} = \left|\frac{i[t_1 + \exp(i\Delta\phi_B)]}{2}\right|^2 \quad (1)$$

where t_1 is the complex transmission amplitude of the two-ring structure given in [2] [the phase of t_1 is shown in Fig. 1(b)], which depend primarily on the round-trip loss in the rings, the reflectivity between the bus and Ring 1 (r_1) and that between Rings 1 and 2 (r_2). In the presence of $\Delta\varphi_B$, the output spectra are asymmetric and the narrow resonances look like Fano resonances [4].

II. Results and Discussion

The 2RMZIs were fabricated in the Electronics and Information Technology Laboratory of the French Atomic Energy Commission (CEA LETI) using a complementary metal–oxide–semicondutor (CMOS)-based 193-nm deep-ultra-violet (UV) process. Fig. 2 shows the 2RMZI and 2R1B devices fabricated in a silicon-on-insulator (SOI) wafer. The SOI consists of 196-nm-thick silicon on a 2-μm-thick buffer oxide layer. The single-mode waveguide has a width of ~450 nm and a measured loss of ~3 dB/cm consistent with [5]. The 3-dB couplers in the MZI are based on multimode interferometers with a width of 3.5 μm and a length of 45 μm. The MZI arms are 200 μm long and are fabricated without any tuning mechanisms. The microring radius is 5 μm for R_1 and 10 μm for R_2. The coupling between the bus and Ring 1 (r_1) and between the rings (r_2) are achieved with "race-track" directional couplers with lengths L_{C1} and L_{C2}, respectively. The outer ring has

TABLE I
2RMZI Devices Under Test (DUTs) Showing the Device Parameters and the Theoretical Fit Parameters. All Length Parameter Is in Micrometers. L_{C3} Are 5, 9, and 13 μm for DUT 01 to 03, Respectively. Note That γ Is the Ratio Between the Circumference of the Outer-Ring (Ring 2) and That of the Inner-Ring (Ring 1)

DUT	γ (fit)	L_{C1}	r_1 (fit)	L_{C2}	r_2 (fit)	n_g (fit)	a_1 (fit)	$\Delta\varphi_B$ (fit)
01	2.000	4	0.86	3	0.90	4.2984	0.995	0.58π
02	2.001	6	0.77	3	0.90	4.272	0.995	0.65π
03	2.000	8	0.65	3	0.90	4.253	0.995	0.61π

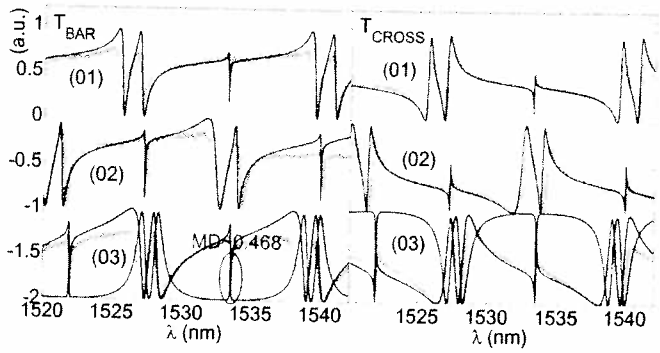

Fig. 3. Measured spectra of 2RMZI bar (in blue) and cross output (in green) for DUT 01 to 03. The faint bold curves are the experimental results, and the solid curves are the theoretical fit. The red curves represent the theoretical case if the bare-MZI is balanced ($\Delta\varphi_B = 0$). The loss factor is measured as $a_1 \sim 0.995$.

two additional straight sections of length of L_{C3}. The gap width is ~200 nm. To facilitate fiber input and output coupling each device is fabricated with vertical grating couplers [6]. The fibers are butt-coupled to the grating couplers at 10° from vertical. The device transmission is measured with a broadband amplified spontaneous emission light source (1.41 to 1.62 μm) and an optical spectrum analyzer. A set of three devices with different L_{C1} values were tested, as listed in Table I.

Fig. 3 shows the measured bar and cross transmission spectra of the 2RMZI devices. The fabricated value of γ for all the devices is close to 2, the condition that gives the maximum finesse for the narrow resonance, which lies in the middle between the two broad resonances. Unfortunately, all the devices exhibit a substantial phase imbalance $\Delta\varphi_B$ between the two MZI arms, thus the narrow resonances resemble the asymmetric Fano resonances rather than the symmetric Lorentzian resonances. Such imbalances are to be expected and difficult to control in a single-batch fabrication [7]. Good theoretical fits based on (1), as shown by the solid curves, can be obtained using the parameter values summarized in Table I, which include the $r_{1,2}$ values, the round-trip amplitude in Ring 1, $a_1 = \exp(-\alpha L_1/2)$, where α is the loss coefficient and L_1 the cavity length, the γ value, the group index, and the phase bias. The $r_{1,2}$ are related to the coupling coefficients (κ_i) of the race-track couplers by $r_i = \sqrt{1-\kappa_i^2}$, and thus r_1 should decrease with increasing coupler length L_{C1}. The r and a values are deduced by fitting the drop output of a standalone 2R1B structure fabricated in the same sample using the formula $D = a\kappa^4/(1 - 2ar^2\cos\delta + a^2r^4)$ [7]. Note that the r is deduced by fitting the Lorentzian lineshape (linewidth), whereas the a value is deduced by matching

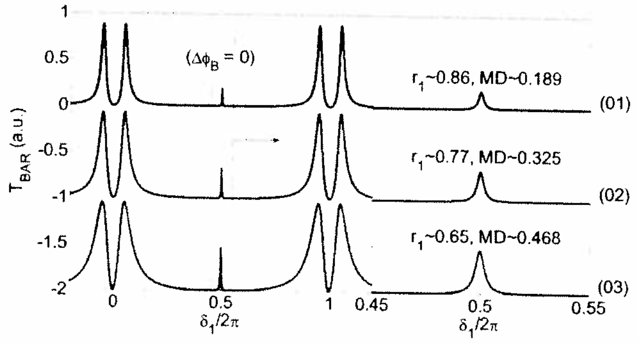

Fig. 4. Bar transmission of 2RMZI using the same parameters as the fabricated DUT 01, 02, and 03 (Table I), assuming balanced MZI ($\Delta\varphi_B = 0$).

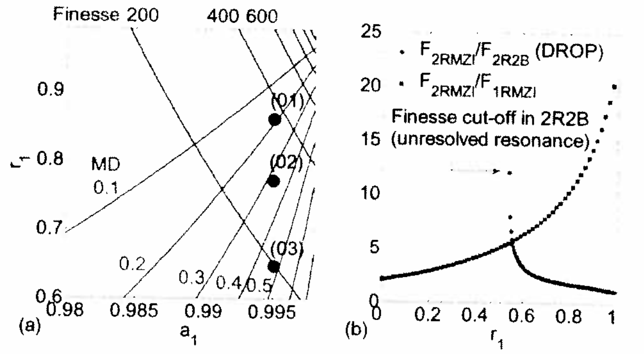

Fig. 5. (a) Finesse (blue)-MD (red) contour plot on which the projected values for the three balanced 2RMZI devices with different r_1 values (given in Table I) are indicated by three circles labeled 1, 2, and 3. (b) Finesse enhancement of 2RMZI relative to the 2R2B and 1RMZI counterparts. In the case of 1RMZI, the r value is assumed to be 0.9. For the 2RMZI and 2R2B, $r_2 \sim 0.9$ and $a_1 \sim 0.995$ are assumed.

the maximum drop output ($D_{\rm MAX}$) of the 1R2B [7]. Finally, the group index of ~4.27 is estimated based on the free-spectral range of the periodic spectra.

Based on the good theoretical fit, we can use the best-fit parameter values to project with some confidence the spectra of the ideal case when the MZI is balanced ($\Delta\varphi_B = 0$), and then compare its performance relative to the 2R2B and 1RMZI structures. Theoretical predictions of the bar output of a balanced MZI ($\Delta\varphi_B = 0$), for the three cases of r_1, while keeping $r_2 \sim 0.9$ and $a_1 \sim 0.995$, are shown in Fig. 4. The three curves show the dependence of the narrow resonance on r_1. The finesse and MD values for the three cases are summarized in the contour plot of Fig. 5(a), which gives the loci of finesse and MD as a function of r_1 and a_1. Similar projections are carried out for 2R2B and 1RMZI, and the finesse of their narrow resonances compared with the 2RMZI device. The relative finesse enhancements of 2RMZI over 2R2B and 1RMZI are shown in Fig. 5(b) as a function of r_1.

Based on these projections for the three values of r_1 that best fit the experiment data, the performance of the three ideal (balanced) 2RMZI devices relative to 2R2B and 1RMZI may be summarized as follows. First, with increasing r_1, the finesse increases while the MD decreases, showing the intrinsic tradeoff between them. For the three cases, $r_1 \sim 0.86$, 0.77, and 0.65, the corresponding finesse values are ~355, 270, and 199, which give the finesse enhancement factor of ~12.4, 9.5, and 7 times relative to the 1RMZI, and of ~1.5, 1.9, and 2.6 times relative to the 2R2B. Note the opposite trends for 1RMZI and 2R2B in their dependence on r_1, as is evident in Fig. 5(b). Compared with 1RMZI, 2RMZI always gives superior finesse. Relative to 2R2B, 2RMZI is superior when r_1 is relatively small. In the high-r_1 regime, the finesse of 2R2B is as good as 2RMZI because the light is so well localized inside the two-ring system, and it becomes insensitive to whether the lower ring is coupled to one or two buses. In terms of MD, 2RMZI gives better results than 2R2B for the lower r_1 values, where the envelope effect dominates and degrades the MD for 2R2B. In the extreme case, the resonance becomes unresolved. On the other hand, for higher r_1 values, the 2RMZI is more sensitive to loss due to higher finesse and the MD can be slightly lower than the 2R2B case. This is a natural occurrence in any high-finesse system. As a guideline, r_1 should be less than ~0.73 for the 2RMZI to have higher MD than the 2R2B (MD ≥ 0.37), in the case where $r_2 \sim 0.9$ and $a \sim 0.995$.

III. Conclusion

We have proposed and demonstrated the 2RMZI device to remove the unwanted envelope effect in the transmission of the 2R2B system [3]. The device is realized on SOI using 193-nm CMOS-based deep-UV lithography. By taking account of the MZI phase imbalance, good agreement is obtained between theory and experimental spectra. Overall, the 2RMZI offers higher finesse and MD compared with the 1RMZI and 2R2B counterparts. In this work, a projected finesse up to 355 with MD ~ 0.19 is realistically achievable by the fabricated 2RMZI devices but only if the fabrication-induced imbalance in the MZI is canceled out either by incorporating width variations in one of the MZI arms or some sort of tuning mechanism (e.g., thermal tuning).

References

[1] J. Heebner, N. Lepeshkin, A. Schweinsberg, G. Wicks, R. Boyd, R. Grover, and P. Ho, "Enhanced linear and nonlinear optical phase response of AlGaAs microring resonators," *Opt. Lett.*, vol. 29, pp. 769–771, 2004.

[2] Y. M. Landobasa, P. Dumon, R. Baets, D. C. S. Lim, and M. K. Chin, "The transmission properties of one-bus two-ring devices," *IEICE Trans. Electron.*, vol. E91-C, no. 2, pp. 167–172, 2008.

[3] Y. M. Landobasa, D. C. S. Lim, P. Dumon, R. Baets, and M. K. Chin, "Finesse enhancement in silicon-on-insulator two-ring resonator system," *Appl. Phys. Lett.*, vol. 92, p. 101122, 2008.

[4] Y. Lu, L. Xu, M. Shu, P. Wang, and J. Yao, "Proposal to produce coupled resonator-induced transparency and bistability using microresonator enhanced Mach–Zehnder interferometer," *IEEE Photon. Technol. Lett.*, vol. 20, no. 7, pp. 529–531, Apr. 1, 2008.

[5] P. Dumon, W. Bogaerts, V. Wiaus, J. Wouters, S. Beckx, J. V. Campenhout, D. Taillaert, B. Luyssaert, P. Bientsman, D. V. Thourhout, and R. Baets, "Low-loss SOI photonic wires and ring resonator fabricated with deep UV lithography," *IEEE Photon. Technol. Lett.*, vol. 16, no. 5, pp. 1328–1330, May 2004.

[6] D. Taillaert, P. Bienstman, and R. Baets, "Compact efficient broadband grating coupler for silicon-on-insulator waveguides," *Opt. Lett.*, vol. 29, pp. 2749–2749, 2004.

[7] S. Darmawan, Y. M. Landobasa, P. Dumon, R. Baets, and M. K. Chin, "Nested-ring Mach–Zehnder interferometer on silicon-on-insulator," *IEEE Photon. Technol. Lett.*, vol. 20, no. 1, pp. 9–11, Jan. 1, 2008.